Theory of two-photon entanglement for spontaneous parametric down-conversion driven by a narrow pump pulse

Timothy E. Keller and Morton H. Rubin
Department of Physics, University of Maryland Baltimore County, Baltimore, Maryland 21250
(Received 9 January 1997)

Spontaneous parametric down-conversion (SPDC) has been extensively studied for the case of a continuous wave pump. In this paper SPDC is studied for the case in which the pump is a pulse. The pump pulse acts like a clock with an uncertainty equal to its width. This makes it possible to distinguish pairs of photons born at sufficiently different depths inside the crystal with a consequent decrease in two-photon interference. We study this effect in detail for degenerate collinear type-II SPDC and degenerate type-I SPDC. It may be possible in the type-II case to eliminate the clock effect of the pump by judicious choice of materials and wavelengths. [S1050-2947(97)00508-8]

PACS number(s): 42.50.Dv, 42.65.Ky, 03.65.Bz

I. INTRODUCTION

Spontaneous parametric down-conversion (SPDC) may be viewed as a coherent three-photon process where a crystal which is not centrosymmetric is illuminated by a pump beam. The pump beam is intense enough to drive the oscillations of the electrons in the crystal into the nonlinear regime. The second order interaction results in the annihilation of a pump photon and the creation of two down-converted photons termed the signal and idler. The photon pairs that are created are entangled in space-time or, equivalently, in wave number and frequency. In most discussions of SPDC the pump has been taken to be monochromatic. This means that the pair can be produced at any time. In this paper the nature of the down-converted photon pairs is studied when the pump is a narrow pulse. This means that the pair can only be produced when the pump pulse is inside the crystal, consequently, the pulse acts like a clock that can be used to distinguish different pairs of the down-converted photons. Since in many two-photon interference experiments, the interference occurs between the amplitudes for pairs born at different times, this distinguishability leads to a decrease in two-photon interference. In type-II SPDC this effect can be eliminanted for certain choices of crystals and pump frequencies.

We shall examine two cases of SPDC. In both cases we shall assume that the signal and idler beams are degenerate, that is, they have the same central frequency. In the type-II case, the pair of photons produced is orthogonally polarized. We will confine our study to the case in which the pair is produced collinearly. In the type I case the signal and idler have the same polarization. The nature of the photon pair produced for nondegenerate type-I is similar to that of the type-II case, but the degenerate type-I case is different, as we shall see.

II. THE INTERACTION HAMILTONIAN AND THE STATE VECTOR

The interaction Hamiltonian describing the down-conversion process [1,2] is given by

$$H_1=\int_V dV\frac{2}{3}\epsilon_0\chi E_i E_s E_p, \tag{1}$$

where χ is the nonlinear electric susceptibility tensor and the integral is over the volume of the crystal. The electric field for the pump, E_p, is taken to be classical, while the signal and idler fields are quantized. The pump beam is linearly polarized and propagating in the z direction. It has a central frequency Ω_p and an envelope of arbitrary shape, $\widetilde{E}_p$. Let

$$\begin{aligned} E_p(z,t)&=e^{-i\Omega_p t}\widetilde{E}_p(z,t),\\ \widetilde{E}_p(z,t)&=\int d\nu_p\overline{E_p}(\nu_p)e^{ik_p(\Omega_p+\nu_p)z-i\nu_p t}. \end{aligned} \tag{2}$$

Using the interaction Hamiltonian, we can now compute the state vector on the output face of the crystal. To first order in the interaction, the state vector for the collinear case is shown in Appendix A to be

$$|\Psi\rangle=|0\rangle+\sum_{k_s,k_i}F(k_s,k_i)a_s^\dagger(k_s)a_i^\dagger(k_i)|0\rangle, \tag{3}$$

where $a^\dagger$ is a photon creation operator and $|0\rangle$ is the vacuum state. The two-photon spectral function is given by

$$F(k_s(\omega),k_i(\omega'))=g\int_{-L}^{0}dz e^{i\Delta(k_s,k_i)z}\overline{E_p}(\omega+\omega'-\Omega_p), \tag{4}$$

where $\Delta(k_s,k_i)=k_p-k_i-k_s$. This differs from earlier work [3] where the pump envelope was a constant. We shall compute this function for the case of both type-I and type-II SPDC.

III. THE TWO-PHOTON AMPLITUDE FOR TYPE-II DOWN-CONVERSION

In type-II SPDC the signal and idler are orthogonally polarized. We shall take the extraordinary ray (e ray) to be the signal and the ordinary ray (o ray) to be the idler. Consider the experiment illustrated in Fig. 1. The beam splitter trans-

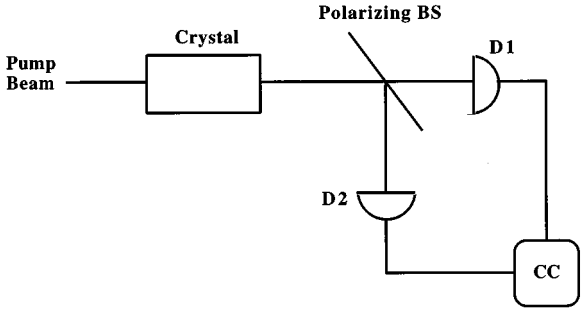

FIG. 1. Simplified two-photon anticorrelation experiment. An intense laser pump beam incident on the crystal produces a pair of orthogonally polarized photons. The pair emerge from the crystal and are split by the polarizing beam splitter, BS. $D1$ and $D2$ are photon detectors and CC is a coincidence counter.

mits the o ray and reflects the e ray. The probability of getting a coincidence count for each pulse is proportional to [4]

$$R_c=\int_0^\infty dT_1\int_0^\infty dT_2\langle\Psi|E_1^{(-)}E_2^{(-)}E_2^{(+)}E_1^{(+)}|\Psi\rangle, \quad (5)$$

where the electric fields are free space fields evaluated at detectors 1 and 2. The field at detector 1 can be written as

$$E_1^{(+)}=\frac{1}{\sqrt{2}}\sum_\omega e_\omega a(k(\omega))e^{-i\omega t_1}, \quad (6)$$

where $a(k)$ is the annihilation operator of a photon with wave number k at the output face of the crystal, $e_\omega=(\hbar\omega/\epsilon_0 V_Q)^{1/2}$, V_Q is the quantization volume, $t_1=T_1-l_1/c$, and l_1 is the optical path length from the output face of the crystal to detector 1. The field E_2 is defined in the same way except there is an extra factor of i multiplying the field because of the reflection from the beam splitter. The expectation value computed using Eq. (3) is

$$\begin{aligned}\langle\Psi|E_1^{(-)}E_2^{(-)}E_2^{(+)}E_1^{(+)}|\Psi\rangle&=|\langle 0|E_2^{(+)}E_1^{(+)}|\Psi\rangle\\&=|A(t_+,t_{12})|^2,\end{aligned} \quad (7)$$

where the two-photon amplitude or biphoton is defined by

$$A(t_+,t_{12})=\langle 0|E_2^{(+)}E_1^{(+)}|\Psi\rangle, \quad (8)$$

where we have introduced the times

$$t_+=\frac{1}{2}(t_1+t_2), \quad (9)$$

$$t_{12}=t_1-t_2. \quad (10)$$

The interpretation of t_{12} is simply the difference in the time of arrival of the idler and signal at the output face of the crystal. If it is positive, the idler arrives after the signal. We may think of t_+ as the time at which the center of momentum of the biphoton arrives at the output face of the crystal.

When frequency filters centered around $\Omega_s=\Omega_i$ are placed in front of the detectors, it is shown in Appendix B that

$$A(t_+,t_{12})=v(t_+)u(t_{12})w(t_+,t_{12}), \quad (11)$$

where

$$v(t)=v_0e^{-i\Omega_p t}, \quad (12)$$

$$u(t)=\Pi(t), \quad (13)$$

$$w(t,t')=\tilde{E}\left(0,t-t'\frac{D_+}{D}\right), \quad (14)$$

and

$$\Pi(t)=\begin{cases}\dfrac{1}{DL} & \text{for} \quad 0<t<DL\\ 0 & \text{otherwise,}\end{cases} \quad (15)$$

$$D=\frac{1}{u_o(\Omega_i)}-\frac{1}{u_e(\Omega_s)}, \quad (16)$$

$$D_+=\frac{1}{2}\left(\frac{1}{u_o(\Omega_i)}+\frac{1}{u_e(\Omega_s)}\right)-\frac{1}{u_p(\Omega_p)}. \quad (17)$$

The $u_r(\Omega)$ are group velocities evaluated at the frequency Ω for beams propagating along the length of the crystal. The v, u, and D functions are the same functions that appear when the pump is a plane wave [3]. When the pump is a plane wave w is a constant, and, because $v(t)$ is a constant times a phase factor, the counting rate is independent of t_+. The width of the biphoton is given by DL, which is the difference in time required for an o ray and an e ray to cross the crystal.

The effect of the finite pulse width of the pump is contained in w, which for type II is given by Eq. (14). Note that D_+L is the difference in time for the center of momentum of the biphoton and the pump to cross the crystal. If we assume that the pump envelope peaks when its argument is zero, we see that the peak of the pump pulse arrives at the output face of the crystal when $t_+=t_{12}D_+/D$. To understand the meaning of this note that when $D_+=0$ the center of the pump pulse arrives at the output face of the crystal at the same time as the center of mass of the biphoton. If $D_+\neq 0$ then the peak of the pulse arrives at a time $|t_{12}D_+/D|$ relative to the center of momentum of the biphoton. If this is a positive number then the peak of the pulse arrives after the center of mass of the biphoton. The magnitude of t_{12}/D may be thought of as the distance from the output face of the crystal to the point at which the biphoton is born. In effect, the pump pulse provides us with a clock with a timing uncertainty equal to the pulse width that can be used to distinguish different biphotons. This leads to a decrease in the indistinguishability that can be observed in two-photon interference experiments. We illustrate this in Fig. 2.

To illustrate the effect of the finite pump width on interference experiments we consider the anticorrelation experiment illustrated in Fig. 3 [5]. We consider the case of a negative uniaxial crystal so the group velocity of the e ray is greater than that of the o ray. As shown in the figure a compensator composed of phase plates is placed immediately after the crystal. The phase plates are oriented so that the o ray travels along the fast axis and the e ray along the

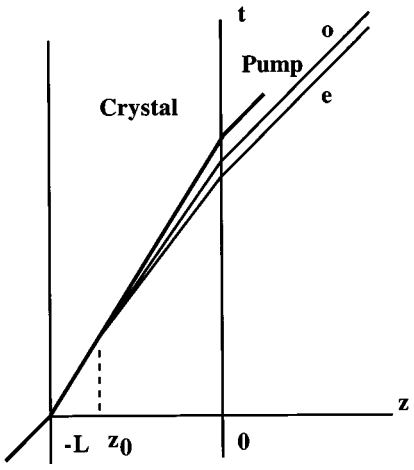

FIG. 2. Feynman diagram for a biphoton. For the case illustrated the biphoton is born at z_0. The e ray leaves the crystal at a time $t=|z_0D|$ ahead of the o ray. In the case of a monochromatic pump, the biphoton pair can be created at any time. For a pulsed pump, it must be created during the time interval when the pump beam is inside the crystal. This localizes the center of momentum of the biphoton. The width of the biphoton is the maximum difference of the times at which the signal and idler photons exit the crystal, DL.

slow axis. In this experiment a 50–50 beam splitter is used. The linear polarizers placed in front of the detectors are oriented at 45° relative to the o and e axes. The biphoton for this case becomes

$$A(t_+,t_{12})=\frac{1}{2}v(t_+)[u(t_{12}+\tau)w(t_+,t_{12}+\tau) - u(-t_{12}+\tau)w(t_+,-t_{12}+\tau)]. \quad (18)$$

When the coincidence counts are computed the v term just gives a constant.

We briefly review the case for which the pump is a plane wave, $w=1$. If the e ray emerges from the crystal before the o ray when there is no compensator, $\tau=0$, there can be no interference because there is no overlap between $u(t_{12})$ and $u(-t_{12})$. The compensator introduces a delay of τ in the e ray relative to the o ray. This causes an overlap between the first and second term in Eq. (18). If the phase delay between the two beams is chosen to be $DL/2$ the coincidences vanish because the overlap between the two terms is complete.

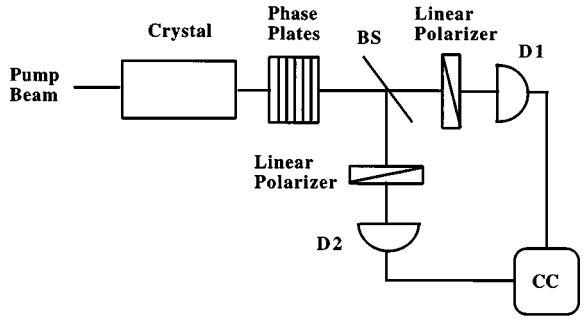

FIG. 3. Type-II two-photon anticorrelation experiment. Phase plates inserted after the crystal have their fast axis parallel to the o ray. By adding plates, the e-ray and o-ray beams may be time shifted relative to one another. Linear polarizers oriented at 45° relative to the e ray are placed in front of the detectors.

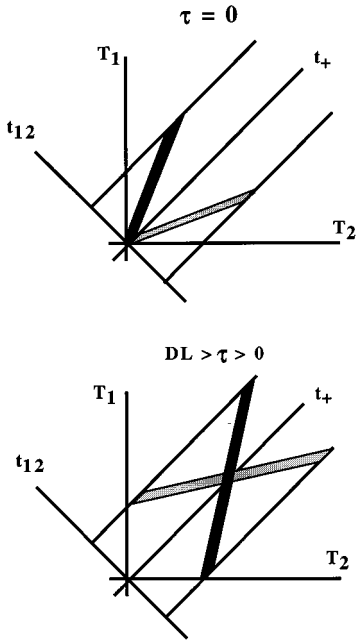

FIG. 4. Illustration of biphoton amplitudes. When $\tau\leqslant 0$ the two parts of the biphoton do not overlap and so cannot interfere. When phase plates oriented as in Fig. 3 are added, the biphoton amplitudes are shifted so that they partially overlap. The width of the pump and the particular values of D and D_+ determine the extent of the overlap. For $DL\leqslant\tau$, the two terms do not overlap and no interference is observed.

In the pulsed pump case this is not true in general because of the presence of w. For complete overlap of the two terms in Eq. (18), it is necessary that $\tau=DL/2$ and equating the arguments of w in the first and second term $t_{12}D_+/D=0$ which requires the vanishing of D_+. This condition is discussed in Appendix D. Figure 4 illustrates the regions in which the two terms of Eq. (18) are nonvanishing.

For a Gaussian pulse envelope,

$$\tilde{E}_p(0,t)=E_p e^{-t^2/2\sigma^2}, \quad (19)$$

we have

$$R_c=\begin{cases} 1-\dfrac{\sigma\sqrt{\pi}}{D_+L}\mathrm{erf}\left(\dfrac{|D_+|L}{\sigma}\dfrac{\tau}{DL}\right), & 0<\tau<\dfrac{DL}{2} \\ 1-\dfrac{\sigma\sqrt{\pi}}{D_+L}\mathrm{erf}\left[\dfrac{|D_+|L}{\sigma}\left(1-\dfrac{\tau}{DL}\right)\right], & \dfrac{DL}{2}<\tau<DL \\ 1 \quad \text{otherwise}, \end{cases} \quad (20)$$

where erf is the error function. Figure 5 shows plots of the coincidence probability for different pulse widths. The example plotted is for BBO with a 350 nm pulse and pulse widths of 10 fs, 100 fs, and 1 ps. The 1 ps pulse is similar to a plane wave pulse in that it gives a ''vee'' shaped dip which goes to zero at $\tau=DL/2$. The effect of the Gaussian in this

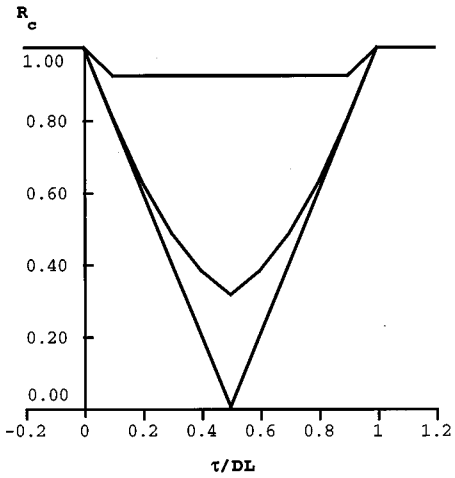

FIG. 5. Plot of Eq. (20) for different pulse widths of 10 fs, 100 fs, and 1 ps for a 1.0-mm BBO crystal with a 350-nm pump. The greater the pulse width the deeper the dip.

case is simply to round off the corners at τ zero and DL. As the pulse width decreases the dip becomes shallower. The depth is found from Eq. (20) by setting $\tau/DL=1/2$. The parameter that determines the depth is the ratio of maximum time delay between the arrival of the pulse and the center of momentum of the biphoton to the pump pulse width, $|D_+|L/\sigma$.

IV. THE TWO-PHOTON WAVE FUNCTION FOR TYPE I

For type-I SPDC the signal and idler photons are created with the same polarization. For the degenerate case this complicates the computation of the biphoton. We begin as before by first computing the biphoton for the case in which the signal goes to detector 1 and the idler goes to detector 2, Fig. 6. In this case, although the signal and idler are again taken to be degenerate, in order to separate them, they are not collinear. We ignore the coordinates transverse to the optical path from the crystal to each detector.

In Appendix C, we show that the biphoton for this case can be written in the form

$$A(t_+,t_{12})=v(t_+)w_I(t_+,t_{12}), \tag{21}$$

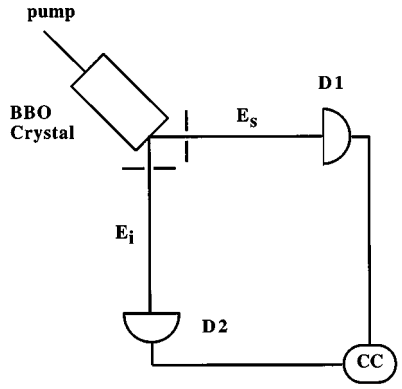

FIG. 6. Type-I experiment. Degenerate pairs of photons are selected by the apertures. In this case the crystal is cut so that these beams are not emitted collinearly.

where v is given by Eq. (12), and t_+ and t_{12} are given by Eqs. (9) and (10).

$$w_I(t_+,t_{12})=\int_{-L}^{0}dz\tilde{E}_p(0,t_++D_+z)\frac{e^{it_{12}^2/4D''z}}{\sqrt{z}}, \tag{22}$$

where for the degenerate case in which the signal and idler are o rays,

$$D_+=\frac{1}{u_o(\Omega_p/2)}-\frac{1}{u_p(\Omega_p)}, \tag{23}$$

and D'' is the dispersion for an o ray evalutated at $\Omega_p/2$,

$$D''=\left.\frac{d^2K_o}{d\Omega^2}\right|_{\Omega=\Omega_p/2}. \tag{24}$$

Equation (22) shows that, if the biphoton is thought of as being created at the point z inside the crystal, the width of the biphoton, described by t_{12}, oscillates and increases because of the dispersion. At the exit face of the crystal the biphoton width is approximately $\sqrt{4|D''z|}$. The length of the biphoton is determined by the pulse width. If the biphoton is imagined to be created at z, its center of momentum, located at t_+, lags or leads the pulse by $|D_+z|$ depending on the sign of D_+.

In our calculations we ignore the dispersion of the pump beam since it will be negligible except for very narrow pump widths. For Gaussian pump envelopes, Eq. (19), and the type of crystals used in SPDC, dispersion will be negligible for $\sigma/\sqrt{L}>20$ fs mm$^{-1/2}$ where L is the length of the crystal. However, we must include dispersion in the calculation of the width of the biphoton for degenerate type-I SPDC. The reason for this is that in the standard Hamiltonian the pair of photons is considered to be created at a single point. If the two photons are nondegenerate the difference in their group velocity will cause them to spread apart and this will determine the width of the biphoton. This is what happens in the type-II case. For the degenerate type-I case the group velocity of the signal and idler is the same and so the width of the biphoton is determined by the next order in the expansion of the wave numbers. As is shown in Appendix C this is just the dispersion of the signal and idler.

To illustrate the effect of the finite pump width on interference, we consider the experiment shown in Fig. 7 [6]. The crystal is cut to provide signal and idler degenerate photons at particular angles which are selected by pinholes. A variable optical delay τ is inserted into the interferometer, which is terminated by a 50–50 beam splitter. In the case of a continuous pump, the state emerging from the beam splitter is of the form $|\psi\rangle=e^{i\omega_i\tau}|i\rangle_t|s\rangle_t-e^{-i\omega_i\tau}|i\rangle_r|s\rangle_r$. The subscripts refer to the case in which both beams are transmitted or both are reflected. We omit the terms which do not lead to coincidences. The negative sign comes from the two 90° phase shifts upon reflection at the beam splitter. For equal optical path lengths, $\tau=0$, the two terms cancel and there are no coincidences [6].

To do the detailed calculation of the biphoton, Eq. (8), the field at each detector must be written in terms of the creation

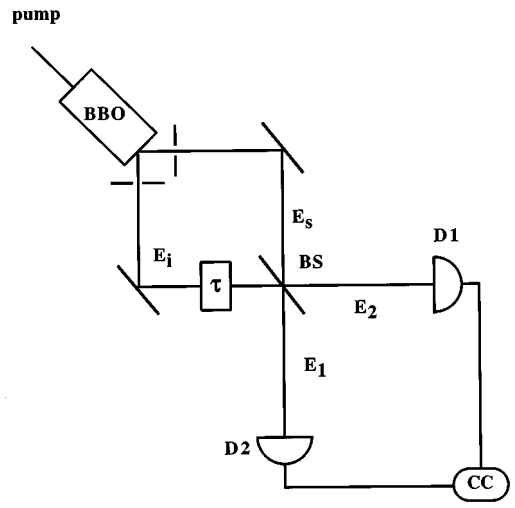

FIG. 7. Type-I HOM [6] experiment. The crystal is cut to provide the signal and idler degenerate photons at two distinct angles which are selected by pinholes. A variable delay τ is introduced into the interferometer. The detection system is the same as in Fig. 1.

and annihilation operators at the output face of the crystal. We again ignore the transverse coordinates,

$$E_1=\frac{1}{\sqrt{2}}\sum_{\omega}\ e_{\omega}[ia_s(k(\omega))+e^{i\omega\tau}a_i(k(\omega))]e^{-i\omega t_1},$$
$$E_2=\frac{1}{\sqrt{2}}\sum_{\omega}\ e_{\omega}[a_s(k(\omega))+e^{i\omega\tau}ia_i(k(\omega))]e^{-i\omega t_2}. \tag{25}$$

In computing the biphoton, we take the signal and idler to be *o* rays and the pump to be an *e* ray inside the crystal. It is shown in Appendix C that the biphoton is

$$A(t_+,t_{12})=\frac{1}{2}v\left(t_+-\frac{\tau}{2}\right)\left[w_{\mathrm{I}}\left(t_+-\frac{\tau}{2},t_{12}-\tau\right)-w_{\mathrm{I}}\left(t_+-\frac{\tau}{2},-t_{12}-\tau\right)\right]. \tag{26}$$

The first term in the square brackets in Eq. (26) corresponds to the case when the signal and idler are transmitted by the beam splitter, while the second term corresponds to their reflection. From this it follows that biphotons that are created farther apart than the pulse width do not interfere because the w_{I} terms in Eq. (26) do not overlap. Alternatively, we may attribute the disappearance of interference to the fact that the two terms in each biphoton are distinguishable by the time their center of momentum leaves the crystal relative to the time the pulse leaves the crystal. Since the pulse is classical, we do not need to worry about any refinements due to the quantum theory of measurement when detecting it.

We can now compute the probability of a coincidence count using Eq. (5):

$$R_c(\tau)=R_c(0)[1-J(\tau)/J(0)], \tag{27}$$

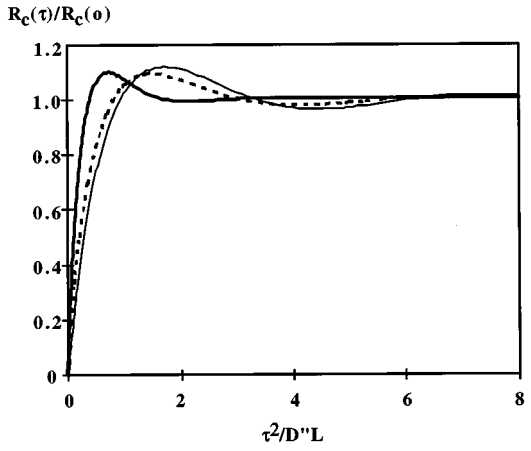

FIG. 8. Plot of $R_c(\tau)/R_c(0)$ defined in Eq. (28) for Gaussian pulses. The three curves are for $(D_+L/2\sigma)^2=0$, 1, and 5. The plane-wave case, $\sigma=\infty$, has the greatest width. The width of the dip decreases as the pulse width decreases. The oscillatory nature is a result of the dispersion of the biphoton.

$$J(\tau)=\mathrm{Re}\int_{-\infty}^{\infty}dt_+\int_{-\infty}^{\infty}dt_{12}w_{\mathrm{I}}(t_+,t_{12}-\tau)w_{\mathrm{I}}^*(t_+,-t_{12}-\tau)$$
$$=\int_{-L}^{0}dz_1\int_{-L}^{0}dz_2\frac{\exp(-i\tau^2/D''\zeta)}{\sqrt{iz_-}}C_p(z_-), \tag{28}$$

where $z_-=z_1-z_2$ and

$$C_p(z_-)=\int_{-\infty}^{\infty}dt_+\tilde{E}_p(0,t_++D_+z_-)\tilde{E}_p^*(0,t_+) \tag{29}$$

is the autocorrelation of the pump envelope. If the pump envelope is taken to be a real Gaussian given by Eq. (19)

$$J(\tau)=J_0\int_0^1 d\zeta\frac{1-\zeta}{\sqrt{\zeta}}\cos\left(\frac{\tau^2}{D''L\zeta}-\frac{\pi}{4}\right)e^{-(D_+L/2\sigma)^2\zeta^2}, \tag{30}$$

where $\zeta=z_-/L$. The function $R_c(\tau)/R_c(0)$ is plotted in Fig. 8 for Gaussian pumps. The physics of $J(\tau)$ may be understood as follows. For $\tau=0$ the cancellation of the two amplitudes in Eq. (26) is always complete because each biphoton created at a given point in the crystal interferes destructively with itself. For $\tau\neq 0$ the interference occurs between the amplitudes for the biphoton created at different times. The exponential term shows that the interference between the amplitudes for pairs created at z_1 and z_2 becomes small when $|D_+||z_1-z_2|$ becomes large compared to the pulse width. As explained above, the pairs created are then distinguishable because their wave packets do not overlap. The quantity $D_+|z_1-z_2|$ measures the different times of arrival of the pairs relative to the clock provided by the pulse. The cosine term comes from the dispersion of the signal and idler beam. For $\tau=0$ the dispersion gives rise to a term $1/\sqrt{D''\zeta}$. The decrease in the interference here is due to the fact that the amplitude for a pair created near the input face of the crystal broadens due to dispersion, while the amplitude for a pair created at the output face does not, therefore the overlap between these amplitudes is less than the overlap

between amplitudes for pairs created nearby to one another. This leads to the decrease in the width of the interference pattern seen in Fig. 8. When we delay the signal relative to the idler, the overlap of the amplitudes oscillates because of the oscillations in the biphoton width.

From Eq. (30) we see that the width of peak is determined by the dimensionless parameters $a=\Delta\tau^2/(D''L)$ and $b=D_+L/(2\sigma)$. From numerical calculations, we have found that the width of the interference pattern, $\Delta\tau$, as measured from the dip to the first maximum is accurately described by

$$1/a^2=c_1b^2+c_2,$$
$$\frac{1}{\Delta\tau^4}=c_1\left(\frac{D_+}{2D''}\right)^2\frac{1}{\sigma^2}+\frac{c_2}{(D''L)^2}, \tag{31}$$

where c_1 and c_2 are numerical constants taken from the numerical calculations. We see that for a steady-state pump, $\sigma\to\infty$, the width of the interference is determined by $\sqrt{D''L}$.

V. CONCLUSION

We have provided a detailed discussion of SPDC for pumps with finite pulse widths. A pump with a finite width was shown to act like a clock with an uncertainty given by the pump width. This allows us to distinguish amplitudes for photon pairs that are born at different depths inside the crystal. Consequently, there is a decrease in two-photon interference effects. For the type-II case this is manifested in a decrease in the visibility for the experiment discussed. In the type-I HOM [6] experiment, the width of the interference dip is decreased. In type-II SPDC, the distinguishability disappears if the crystal and the wavelengths can be chosen so D_+, defined in Eq. (17), vanishes. The physics of degenerate type-I SPDC is different from that of type II and nondegenerate type I. In degenerate type I the width of the biphoton is determined by dispersion and is inherently narrower than the other cases. This may have advantages in preparing entangled four-photon states [11].

ACKNOWLEDGMENTS

We have benefited from many discussions with Y. H. Shih and T. Pittman for which we wish to express our gratitude. This work was supported, in part, by the U.S. Office of Naval Research, Grant No. N00014-91-J-1430.

APPENDIX A: STATE VECTOR

We begin with a linearly polarized input pulse propagating in the z direction. The pump has a central frequency Ω_p and an envelope of arbitrary shape, $\tilde{E}_p$, given by Eq. (2).

The interaction Hamiltonian (1) may be written using the rotating wave approximation as

$$H_1=\int_V dxdydz\left(-\frac{2}{3}\epsilon_0\chi E_i^{(-)}E_s^{(-)}E_p^{(+)}+\text{H.c.}\right), \tag{A1}$$

where χ is the nonlinear electric susceptibility tensor, and H.c. stands for the Hermitian conjugate. In defining the signal and idler field, we confine ourselves to the collinear case. The signal field is defined by

$$E_s^{(+)}=\sum_\omega\frac{e_\omega}{n_s(\omega)}a_s(k_s(\omega))e^{i[k_s(\omega)z-\omega t]}, \tag{A2}$$

where $a_s(k_s(\omega))$ is the annihilation operator for the signal mode with frequency ω,

$$k_s(\omega)=n_s(\omega)\omega/c, \tag{A3}$$

n_s is the index of refraction of the signal beam, c is the speed of light,

$$e_\omega=\sqrt{\frac{\hbar\omega}{2\epsilon_0V_Q}}, \tag{A4}$$

and V_Q is the quantization volume. The idler field is defined in an analogous fashion. The pump beam may be treated classically.

The state vector is computed using first order perturbation theory [3]. In the interaction picture, we have

$$|\Psi\rangle=|0\rangle-\frac{i}{\hbar}\int_{-\infty}^{\infty}H_1(t)dt|0\rangle. \tag{A5}$$

Substituting the expressions for the fields into this expression we can compute the spectral function Eq. (4).

APPENDIX B: TYPE II-EQUATIONS

We consider the experiment illustrated in Fig. 1. The biphoton defined in Eq. (8) is given by

$$A(t_+,t_{12})=\frac{i}{2}\sum_{\omega,\omega'}e_\omega e_{\omega'}e^{-i\omega t_1}e^{-i\omega' t_2}F(k_s(\omega),k_i(\omega')), \tag{B1}$$

where t_+ and t_{12} are defined in Eqs. (9) and (10).

1. Phase matching

Suppose the crystal is cut so that

$$\Omega_s+\Omega_i=\Omega_p, \tag{B2}$$
$$K_s+K_i=K_p, \tag{B3}$$
$$K_r=n_r\Omega_r/c,\quad r=s,i,p. \tag{B4}$$

Now let $\omega=\Omega_i+\nu_i$, $\omega'=\Omega_s+\nu_s$, and $\omega_p=\Omega_p+\nu_p$ where, even for femtosecond pulses, we may assume that the $|\nu_r|\ll\Omega_r$. Using these results, we have to first order

$$k_r=K_r+\frac{\nu_r}{u_r(\Omega_r)}, \tag{B5}$$

where $u_r(\Omega_r)$ is the group velocity of the r beam.

We now compute $\Delta(k_s,k_i)$ to first order,

$$\Delta(k_s,k_i)=k_p-k_i-k_s, \tag{B6}$$

$$\Delta(k_s,k_i)=K_p-K_i-K_s+\frac{\nu_p}{u_p(\Omega_p)}-\frac{\nu_i}{u_i(\Omega_i)}-\frac{\nu_s}{u_s(\Omega_s)}. \tag{B7}$$

When we use Eq. (B3) and the fact that $\nu_p=\nu_s+\nu_i$, we find that

$$\Delta(k_s,k_i)=-\left(\nu_pD_++\frac{1}{2}\nu_-D\right), \tag{B8}$$

where

$$\nu_-=\nu_i-\nu_s, \tag{B9}$$

$$D=\frac{1}{u_i(\Omega_i)}-\frac{1}{u_s(\Omega_s)}, \tag{B10}$$

$$D_+=\frac{1}{2}\left(\frac{1}{u_i(\Omega_i)}+\frac{1}{u_s(\Omega_s)}\right)-\frac{1}{u_p(\Omega_p)}. \tag{B11}$$

2. Evaluation of the type-II biphoton

We can now evaluate the biphoton

$$A(t_+,t_{12})=v_1e^{-i\Omega_pt_+}I, \tag{B12}$$

where the slowly varying quantities have been absorbed into v_1 and

$$I=\int_{-L}^{0}dz\int_{-\infty}^{\infty}d\nu_-\int_{-\infty}^{\infty}d\nu_pe^{-i(1/2)\nu_-(t_{12}+Dz)}\times e^{-i\nu_p(t_++D_+z)}\overline{E_p}(\nu_p). \tag{B13}$$

The integral over ν_- gives a Dirac δ function of argument $Dz+t_{12}$ which may be interpreted by saying that if a pair is created at the point z inside the crystal, $-L<z<0$, for D positive, the idler will be detected at a time $D|z|$ after the signal. This is the case for a negative uniaxial crystal where the group velocity of the o ray is less than that of the e ray. We can now write

$$A(t_+,t_{12})=v(t_+)u(t_{12})w(t_+,t_{12}), \tag{B14}$$

where

$$v(t)=v_0e^{-i\Omega_pt}, \tag{B15}$$

$$u(t)=\Pi(t), \tag{B16}$$

$$w(t,t')=\tilde{E}\left(0,t-t'\frac{D_+}{D}\right), \tag{B17}$$

and

$$\Pi(t)=\begin{cases}\dfrac{1}{DL} & \text{for} \quad 0<t<DL\\ 0 & \text{otherwise.}\end{cases} \tag{B18}$$

APPENDIX C: TYPE-I EQUATIONS

Consider the experiment illustrated in Fig. 6. The signal and idler beams are not collinear; however, we shall assume that they emerge at small angles so that we can ignore transverse walkoff effects. In addition, we assume that we can ignore the coordinates that are transverse to the optical path lengths. The effects of these coordinates for a steady-state pump have been discussed in [7]. Using Eqs. (8), (3), and (4) we obtain

$$A(t_+,t_{12})=g\sum_{k_s,k_i}\int_{-L}^{0}dze^{i\Delta(k_s,k_i)z}\overline{E_p}(\omega_s+\omega_i-\Omega_p)\times e^{-i(\omega_it_1+\omega_st_2)}e^{i\omega_i\tau}, \tag{C1}$$

where the arguments of A are related to t_1 and t_2 by Eqs. (9) and (10). As usual, all the slowly varying factors are absorbed into g.

1. Phase matching

Following the path set out in Appendix B we assume that the crystal has been cut so Eqs. (B2)–(B4) hold. The signal and idler beams are not collinear, however, we ignore the transverse coordinates. Furthermore, in this case we shall assume that the signal and idler are degenerate, $\Omega_s=\Omega_i=\Omega_p/2$, and that they are o rays. Introduce $\omega_i=\Omega_i+\nu_i$, $\omega_s=\Omega_s+\nu_s$, and $\omega_p=\Omega_p+\nu_p$ and substitute them into Eq. (B7). Using the definitions $\nu_s+\nu_i=\nu_p$ and $\nu_-=\nu_i-\nu_s$, we find that the first order dependence in ν_- is not present because D defined in Eq. (B10) vanishes. Therefore it is necessary to carry out the expansion of the wave numbers (B5) to higher order to get the leading term in ν_-. For $r=s,i$,

$$k_r=K_o+\frac{\nu_r}{u_o(\Omega_p/2)}+\frac{1}{2}D''\nu_r^2, \tag{C2}$$

where D'' is the dispersion for an o ray evaluated at $\Omega_p/2$,

$$D''=\left.\frac{d^2K_o}{d\Omega^2}\right|_{\Omega=\Omega_s}. \tag{C3}$$

This gives

$$\Delta(k_s,k_i)=-\left(\nu_pD_++\frac{1}{4}\nu_-^2D''\right), \tag{C4}$$

with D_+ defined in Eq. (17). The second order term in ν_p may be neglected since it is small compared to the first term for the crystal lengths used in typical experiments. Since the signal and idler group velocities are equal, D_+ reduces to the result given in Eq. (23).

2. Evaluation of the type-I biphoton

Substituting Eq. (C4) into Eq. (C1) and converting the sums over the wave numbers to integrals over the frequency gives

$$A(t_+,t_{12})=\frac{1}{2}ge^{\Omega_p(t_+-\tau/2)}\int_{-L}^{0}dz\int_{-\infty}^{\infty}d\nu_-$$
$$\times\int_{-\infty}^{\infty}d\nu_p e^{-i[\nu_p D_+ +(1/4)\nu_-^2 D'']z}\overline{E_p}(\nu_p)$$
$$\times\{e^{-i\nu_p(t_+-\tau/2)}e^{-i(\nu_-/2)(t_{12}-\tau)}-(t_1\leftrightarrow t_2)\}. \tag{C5}$$

We can now write the biphoton in the form (26) with

$$w_I(t,t')=\int_{-L}^{0}dz\int_{-\infty}^{\infty}d\nu_p$$
$$\times\int_{-\infty}^{\infty}d\nu_- e^{-i[\nu_p D_+ +(1/4)\nu_-^2 D'']z}$$
$$\times\widetilde{E}_p(\nu_p)e^{-i\nu_p t}e^{-i(1/2)\nu_- t'}. \tag{C6}$$

Evaluating the integral over the frequencies and putting the irrelevant constants in v gives Eq. (22).

APPENDIX D: D_+ CALCULATION

This appendix illustrates how material selection and the choice of a suitable pump frequency can eliminate the clock effect of the pump for type-II SPDC. This occurs if D_+, defined in Eq. (17), vanishes. We refer to this as group velocity matching, i.e., the inverse of the pump group velocity equals the mean of the idler and signal inverse group velocity. Consequently, the center of momentum of the biphoton and the center of pump pulse arrive at the exit face of the crystal at the same time.

For a uniaxial birefringent crystal, we take the signal photon to have extraordinary polarization and the idler photon to have ordinary polarization [8]. The wave vectors are

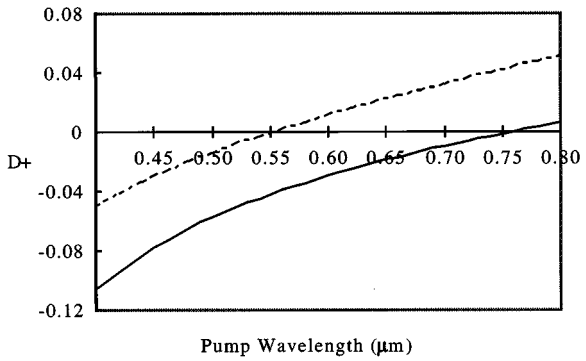

FIG. 9. D_+ is plotted as a function of the pump central wavelength. The wavelength at which the group velocity matching condition, $D_+=0$, is satisfied is 0.54 nm for KDP (dashed curve) and 0.75 nm for BBO (solid curve).

$$k_o(\lambda)=\frac{2\pi n_o(\lambda)}{\lambda},\quad k_e(\lambda)=\frac{2\pi N_e(\lambda,\gamma)}{\lambda},$$

$$N_e^2(\lambda,\gamma)=\left(\frac{\gamma^2}{n_o^2(\lambda)}+\frac{1-\gamma^2}{n_e^2(\lambda)}\right), \tag{D1}$$

with $\gamma=\cos\theta$ where θ is the angle between the crystal optical axis and the z axis and n_o and n_e are the principal refractive indices.

The phase matching equations are iterated for a given wavelength to determine the angle θ between the optical axis and the z direction (remember this is the collinear case.) Then, D_+ is calculated. Plots for two different materials, BBO [9] and potassium dihydrogen phosphate (KDP) [10], are shown in Fig. 9.

[1] W. H. Louisell, A. Yariv, and A. E. Siegman, Phys. Rev. **124**, 1646 (1961).
[2] D. N. Klyshko, *Photons and Nonlinear Optics* (Gordon and Breach Science Publishers, New York, 1988).
[3] M. H. Rubin, D. N. Klyshko, Y. H. Shih, and A. V. Sergienko, Phys. Rev. A **50**, 5122 (1994).
[4] R. J. Glauber, Phys. Rev. **130**, 2529 (1963); **131**, 2766 (1963).
[5] A. V. Sergienko, Y. H. Shih, and M. H. Rubin, J. Opt. Soc. Am. B **40**, 859 (1993).
[6] C. K. Hong, Z. Y. Ou, and L. Mandel, Phys. Rev. Lett. **59**, 2044 (1987).
[7] M. H. Rubin, Phys. Rev. A **54**, 5349 (1996).
[8] M. Born and E. Wolf, *Principles of Optics*, 6th ed. (Pergamon Press, Oxford, 1980).
[9] Beta Barium Borate Product Handbook, Basic Properties, Advantages, and Major Applications (Fujian Castech Crystals, Inc., Fuzhou Fujian, P.R. China).
[10] F. Zernike, J. Opt. Soc. Am. **54**, 1215 (1964).
[11] See, for example, Y. H. Shih and M. H. Rubin, Phys. Lett. A **182**, 16 (1993); M. Zukowski, A. Zeilinger, M. A. Horne, and A. K. Ekert, Phys. Rev. Lett. **71**, 4287 (1993); M. Pavičić J. Opt. Soc. Am. B **12**, 821 (1995); M. Zukowski, A. Zeilinger, and H. Weinfurter, Ann. (N.Y.) Acad. Sci. **755**, 91 (1995).